J Mater Sci (2008) 43:1510–1514
DOI 10.1007/s10853-007-2374-3

Titanate nanotubes: preparation, characterization, and application in the detection of dopamine

Liling Niu · Mingwang Shao · Sheng Wang · Lei Lu · Huazhong Gao · Jun Wang

Received: 11 July 2007 / Accepted: 3 December 2007 / Published online: 1 January 2008

Abstract Titanate nanotubes were successfully synthesized via a hydrothermal process with the assistance of surfactant. These nanotubes with average length of several hundred nanometers and diameter of 10 nm were employed to modify glass carbon electrode and measure dopamine via electrochemistry method. The experiments showed ideal reversibility in cyclic voltammetry, which might be due to the decrease of the overvoltage of the electrode and increase of electron transference. The results illustrated the potential application in the detection of dopamine.

Introduction

The fabrication of one-dimensional nanomaterials, such as nanowires, nanorods, nanotubes, and nanoribbons has been intensely studied because of the promising applications of these materials in various fields of technology. Following the discovery of carbon nanotubes (CNTs) [1], a series of metal oxide nanotubulars were successfully synthesized as potentially useful materials, for example, nanotubes of ceramic oxides containing Al, V, Si, and Mo [2], surfactant-intercalated VO_x [3] and crystalline titanium oxide [4, 5]. These nanotubes were inimitable one-dimensional nanostructures with high specific surface area and uniform nanometer-sized channels possessing electronic conductivity.

L. Niu · M. Shao (✉) · S. Wang · L. Lu · H. Gao · J. Wang
Anhui Key Laboratory of Functional Molecular Solids, and College of Chemistry and Materials Science, Anhui Normal University, Wuhu 241000, P.R. China
e-mail: mwshao@mail.ahnu.edu.cn

Dopamine (DA) is one of the most important catecholamines and belongs to the family of inhibitory neurotransmitters [6]. Low level of DA has been found in patients with Parkinson's disease. For this purpose, DA was detected with various modified electrodes, such as, CNT-film-modified electrode [7], Nafion [8], negatively charged film [9], and nanoparticle film [10] electrodes. Recently, the titanate nanotube (TNT) membrane attracted intensive intention in the voltammetrical detection of DA with a TNT-membrane covered glass carbon electrode (GCE). However, the TNT/GCE made DA exhibit a quasi-reversible electrochemical reaction at the electrode surface, which results in a peak-to-peak separation of 130 mV at a scan rate of 50 mV s^{-1} [11].

Herein, sodium dodecyl sulfate (SDS) was employed in the hydrothermal synthesis of TNTs, which were employed to modify GCE. This TNT/GCE exhibited a good reversible redox peaks in the detection of DA and showed to be a useful biosensing surface to detect DA.

Experimental procedure

Synthesis of TNTs

The TNTs were prepared as follows: adding anatase TiO_2 powder (0.428 g, diameter less than 0.1 mm) and SDS (0.5 g) to an aqueous solution of NaOH (50 mL, 10 M), after vigorously stirring for 1 h and ultrasonic irradiating for another 1 h (SK1200H, 45 W), the milky suspension was transferred into a Teflon-lined autoclave and heated to 140 °C for 72 h. The resultant was neutralized by dilute nitric acid solution and then aged in pH ~2 conditions for 12 h at room temperature. The resulting white products were filtered, then washed with absolute ethanol and

distilled water for several times, finally dried in vacuum oven at 60 °C for 12 h.

Preparation of TNT/GCE

Put TNT powder (0.01 g) in 5 mL *N*,*N*-dimethylformamide and sonicate to get TNT suspension.

GCE ($\Phi = 2$ mm) was polished with a 0.05 μm alumina slurry and washed with water in an ultrasonic bath for a few minutes. After washing with sonication, the GCE was coated with 10 μL TNT suspension, and *N*,*N*-dimethylformamide was allowed to evaporate at room temperature.

Characterization

The phase and the crystallography of the products were characterized from an X-ray diffraction (XRD) pattern, which was recorded by using a Shimadzu XRD-6000 X-ray diffractometer equipped with Cu Kα radiation ($\lambda = 0.15406$ nm), was applied to record the pattern in the 2θ range of 5–80°.

The morphology and microstructure of the samples were analyzed using a scanning electron microscope (SEM) (Hitachi S-4800) equipped with an energy dispersive spectrum (EDX), transmission electron microscope (TEM) (Hitachi H-800) spectroscope, and a high-resolution transmission electron microscope (HRTEM) (JEOL-2010, 200 kV), respectively. TG-DTA measure was performed in SETARAM-TGA92 in the temperature range from room temperature to 900 °C at heating rate of 10 °C min^{-1}. Raman spectrum was performed with a Labram-HR confocal laser microRaman spectrometer; an argon-ion laser excitation at 514.5 nm was used.

Electrochemical experiments were performed with electrochemistry workstation (CHI 620B, ChenHua Instruments Co.) with a three conventional electrode system. The TNT/GCE was used as working electrode. A saturated calomel electrode (SCE) and a platinum wire were used as the reference electrode and the counter electrode, respectively.

Result and discussion

SEM image (Fig. 1) gives a general view of the as-prepared products in a large quantity of tubular-like structures. These nanotubes were slightly curved with the length of several hundred nanometers. The EDX indicates the sample that mainly consists of Ti and O peaks with the atomic ratio of 1:2. The C peak is from the surface adsorption and Au peak is from the sample sputter coated with gold before the SEM investigation. And there also exists a weak peak of Na in the spectrum with the Na:Ti atomic ratio of 1:9.73, which indicates that TNTs are mainly H-titanate.

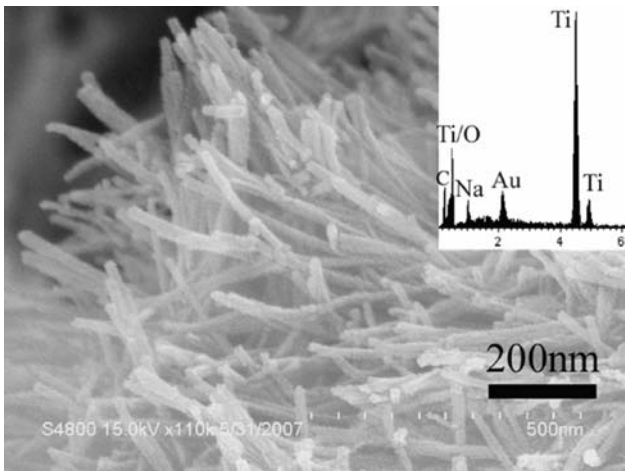

Fig. 1 SEM image of large-scale TNTs and the EDX spectrum (inset) revealing their chemical composition

Figure 2 shows the XRD pattern of the products, which is similar to titanate reported before [12, 13]. All diffraction peaks can be indexed by the orthorhombic system with the lattice constants, $a = 0.1803$ nm, $b = 0.33784$ nm, and $c = 0.2998$ nm (JCPDS card. 47-0124). Since the TNTs are slightly curved (Fig. 1), the diffraction peaks related to the *Z*-axis (e.g. (301), (501), (002)) are much weaker than the peaks (200), (110), (600), and (020) [14].

The morphology and structure of the products were further examined with TEM images. Figure 3a shows the typical TEM microstructure of the TNTs with average outer/inner diameter of 9/4.4 nm. The nanotubes contain open-ended tubular structure. Figure 3b is the TEM image with large magnification which indicates that the prepared nanotubes are uniform.

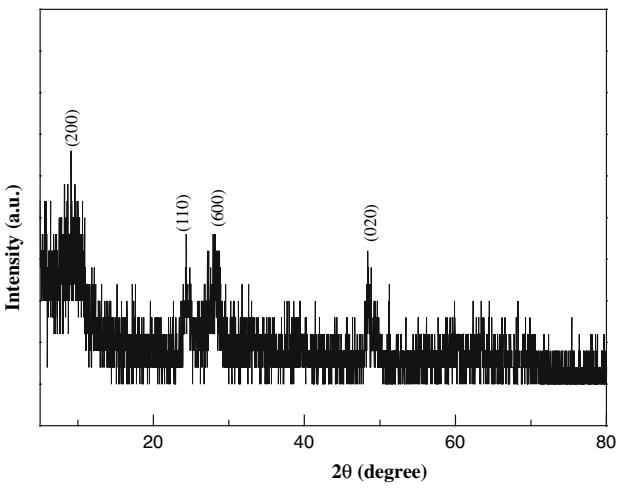

Fig. 2 XRD pattern of the as-prepared products

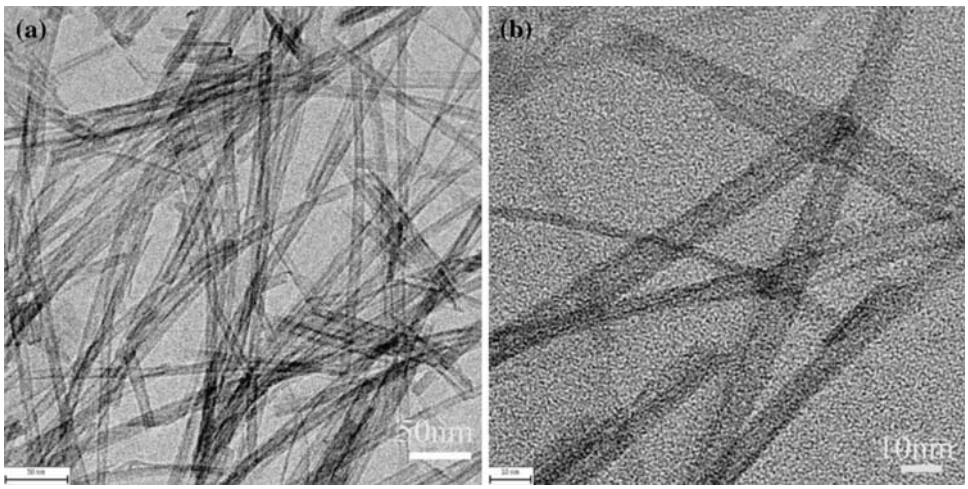

Fig. 3 TEM image of TNTs (**a**) low and (**b**) large magnification

Detailed structures of the nanotubes were investigated by selected-area electron diffraction (SAED) and HRTEM (Fig. 4). The tubes were not single crystalline judged from the HRTEM image. SAED pattern shows diffraction rings indexed as (110), (020). HRTEM and SEAD confirm that TNTs are polycrystalline.

Thermo-gravimetric analysis (Fig. 5) was performed in a TGA-DTA system, about 17% weight loss of the as-prepared nanotube is mainly due to the H-titanate decomposed into TiO_2 and H_2O, as well as some surface adsorbed H_2O, which indicates that the as-prepared nanotube to be $Na_xH_{2-x}Ti_2O_5{\cdot}H_2O$ ($x = 0.2$).

FTIR spectrum was characterized and investigated the existence of SDS on the TNTs, Fig. 6 is the FTIR spectrum of the as-prepared products. The band at 2,958 cm^{-1} is

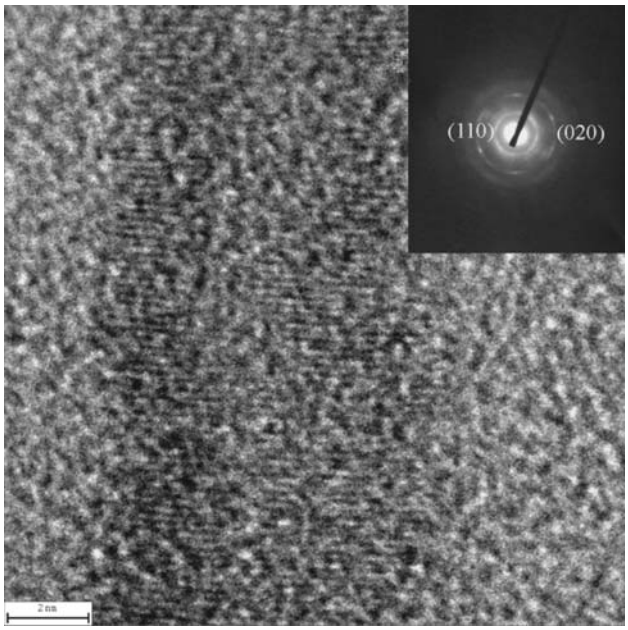

Fig. 4 HRTEM image of TNT and its SAED (inset) showing diffraction rings

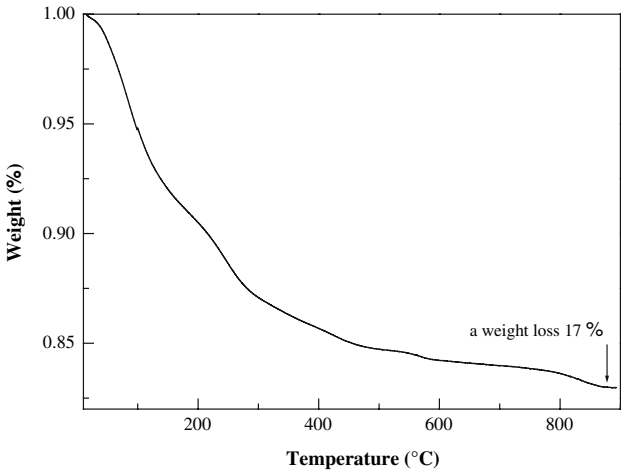

Fig. 5 Thermal-gravity analysis plot of TNTs revealing weight loss of 17%

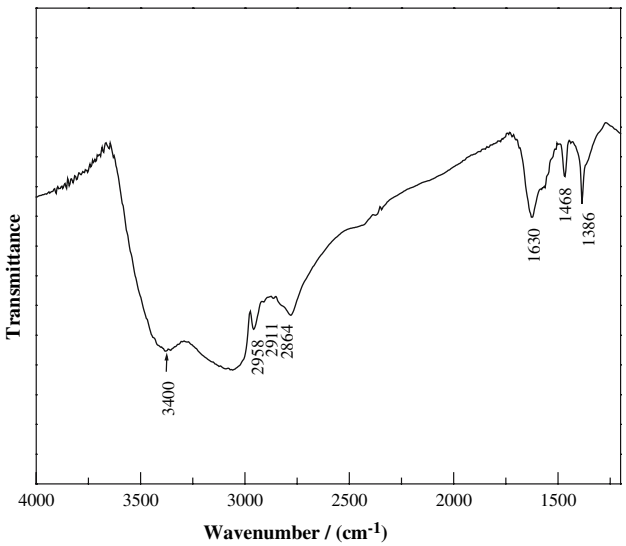

Fig. 6 FTIR spectrum of TNTs containing SDS

assigned to the asymmetrical stretching of $-CH_3$. The bands at 2,911 and 2,864 cm^{-1} are due to asymmetrical and symmetrical stretching of $-CH_2-$, respectively. The asymmetrical and symmetrical bending vibrations of $-CH_3$ are represented at 1,386 and 1,468 cm^{-1} [15]. All the above bands indicate the existence of SDS. And the bands at 1,630 and 3,400 cm^{-1} are attributed to a binding vibration of H–O–H and O–H, respectively, which demonstrate the existence of water and hydroxyl groups on the TNTs [12].

The Raman spectrum of TNTs (Fig. 7) was similar to that reported by Kasuga et al. [5]. The peak at 280 cm^{-1} was suggested to be duo to Na–O–Ti, as report for Na_2O-TiO_2 glass in accord with the EDX results [16]. The peak seen at 450 cm^{-1} was due to Ti–O–Ti [17]. The peaks at about 670–760 cm^{-1} were duo to the Ti–O–Ti stretch in edge-shared TiO_6 [18].

Figure 8 plots the cyclic voltammograms (CVs) in 0.1 M phosphate buffer solution (PBS) containing 4.74×10^{-4} M DA. At the bare GCE (Fig. 8a), a couple of quasi-reversible redox peaks were observed and the peak-to-peak separation (ΔEp) was 192 mV. The TNT/GCE enhanced the redox peak currents of DA compared with the bare GCE (Fig. 8b). The separation between peak potentials was 43 mV. The results show that TNT/GCE not only enhanced the redox peak currents but also made the redox reaction of DA more reversible. When TNT without SDS/GCE was employed, the peak currents are the most while reversible is the worst of the three electrodes as shown in Fig. 8c, which indicates that the negative surface charge of TNTs may adsorb cation [19]. Compared with the TNT without SDS/GCE, the results of TNT/GCE indicate that the anionic surfactant of SDS increases the reversible of this electrochemistry.

In order to obtain a better resolution among the voltammograms, square-wave voltammogram (SWV) has been employed. As shown in Fig. 9, it depicts SWVs of a

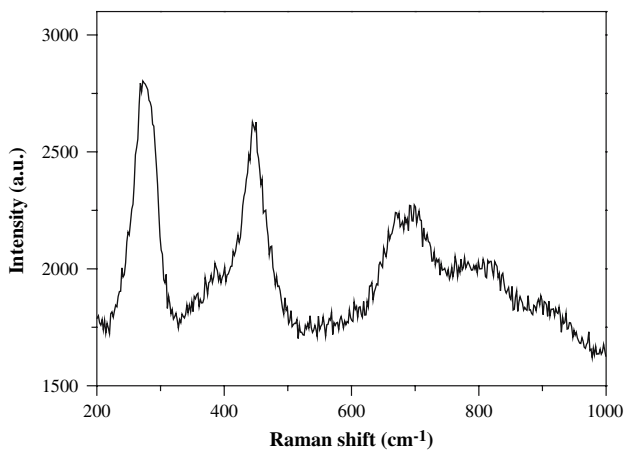

Fig. 7 Raman spectrum of TNTs

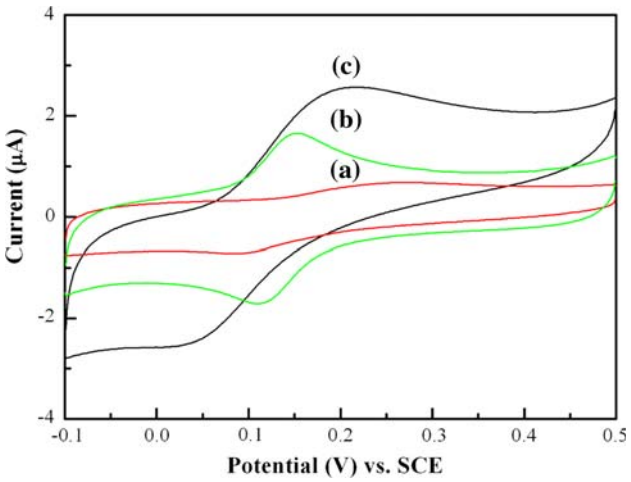

Fig. 8 CVs of 4.74×10^{-4} M DA in 0.1 M phosphate buffer solution (PBS pH 7.4) with scan rate of 50 mV s^{-1}: (**a**) bare GCE, (**b**) TNT/GCE, and (**c**) TNT without SDS/GCE

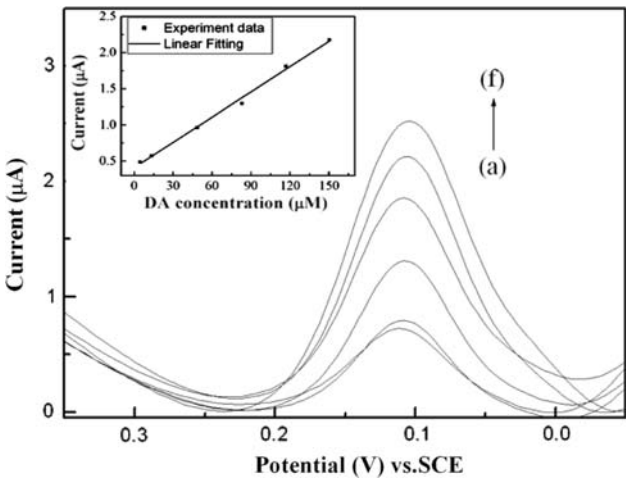

Fig. 9 SWV with correction of background current for different concentration of DA with TNT/GCE in a pH 7.4 phosphate buffer; and the linear plot of peak current vs. different concentration of DA: (**a**) 4.45 μM, (**b**) 13.35 μM, (**c**) 48.47 μM, (**d**) 83 μM, (**e**) 116.9 μM, and (**f**) 150.3 μM (inset)

physiological solution determining DA at TNT/GCE while changing DA concentration in PBS (pH 7.4). A series of well-defined peaks for DA are obtained owing to its good reversibility. After the correction of the background current, the detection limit of DA is calculated as 1.0×10^{-7} M, and the linear calibration graph is obtained over the DA concentration range 4.45×10^{-6} to 1.55×10^{-4} M. The linear equation is $i_{pa} = 0.410 + 0.011C_{DA}$ with the correlation coefficient of 0.9979.

Compared with the bare GCE (Fig. 8a), TNT/GCE (Fig. 8b) enhanced the redox peak currents of DA. This phenomenon implies that the as-prepared products can improve the electron transfer between DA and the GC electrode. It should be ascribed to tube's structure with a

nanometer-scale inner-core cavity exposed to the outer surface [20] and the negative surface charge. The surfactant SDS is important because it can reduce the overvoltage of the electrode and increase the rate of electron transfer [21], which results in a better reversibility in the electrochemical detection.

Conclusion

A large quantity of TNTs were successfully synthesized via a hydrothermal process with the assistance of surfactant SDS. The observation of the nanotubes structure showed that it was polycrystalline. Compared with the bare GCE and the TNT/GCE without SDS, the TNT/GCE makes DA exhibit a reversible electrochemical reaction at the electrode surface. And surfactant SDS relatively improved the reversibility in the cyclic voltammetry of TNT/GCE.

Acknowledgements Financial support from the National Natural Science Foundation of China (20571001), the Education Department (No. 2006KJ006TD) of Anhui Province and Anhui Provincial Natural Science Foundation (070414185) are appreciated.

References

1. Iijima S (1991) Nature 354:56
2. Niederberger M, Muhr HJ, Krumeich F, Bieri F, Gunther D, Nesper R (2000) Chem Mater 12:1995
3. Satishkumar BC, Govidaraj A, Vogl EM, Basumallick L, Rao CNR (1997) J Mater Res 12:604
4. Kasuga T, Hiramatsu M, Hoson A (1998) Langmuir 14:3160
5. Kasuga T, Hiramatsu M, Hoson A, Sekino T, Niihara K (1999) Adv Mater 11:1307
6. Phillips PEM, Stuber GD, Heien MLAV, Wightman RM, Carelli RM (2003) Nature 422:614
7. Shao MW, Li M, Ban HZ, Niu LL, Wang H, Pan SY (2007) J Mater Sci 42: 6961
8. Lacroix M, Bianco P, Lojou E (1999) Electroanalysis 11:1068
9. Kawagoe KT, Zimmerman JB, Wightman RM (1993) J Neurosci Methods 48:225
10. Yuan S, Hu S (2004) Electrochim Acta 49:4287
11. Liu AH, Wei MD, Honma I, Zhou HS (2006) Adv Funct Mater 16:371
12. Sun XM, Li YD (2003) Chem Eur J 9:2229
13. Ma R, Bando Y, Sasaki T (2003) Chem Phys Lett 380:577
14. Sasaki T, Watanabe M, Komatsu Y, Fujiki Y (1985) Inorg Chem 24:2265
15. Jiang LQ, Gao L, Sun J (2003) J Colloid Interf Sci 260:89
16. Kim HM, Miyaji F, Kokubo T, Nakamura T (1997) J Mater Sci Mater Med 8:341
17. Manuel O, Garcia-Ramos JV, Serna CJ (1992) J Am Ceram Soc 75:2010
18. Su Y, Balmer ML, Bunker BC (2000) J Phys Chem B 104:8160
19. Bavykin DV, Milsom EV, Marken F, Kim DH, Marsh DH, Riley DJ, Walsh FC, El-Abiary KH, Lapkin AA (2005) Electrochem Commun 7:1050
20. Chen Q, Zhou W, Chen Q, Du G, Peng L (2002) Adv Mater 14:1208
21. Zheng JB, Zhou XL (2007) Bioelectrochemistry 70:408